Welding International
Vol. 24, No. 4, April 2010, 258–265
Selected from *Soldagem & Inspeção* 2008 13(3) 237–244

Taylor & Francis
Taylor & Francis Group

Effect of post-weld heat treatment on the wear resistance of hardfacing martensitic steel deposits

Agustín Gualco[a1], Hernán G. Svoboda[b2], Estela S. Surian[a,c3] and Luis A. de Vedia[d4]

[a]*Faculty of Engineering, Universidad Nacional de Lomas de Zamora, Buenos Aires, Argentina;* [b]*Materials and Structures Laboratory, Faculty of Engineering, Conicet, Universidad de Buenos Aires, Buenos Aires, Argentina;* [c]*Deytema-Centre for Materials Development and Technology, Regional Faculty of San Nicolás, Universidad Tecnológica Nacional, Buenos Aires, Argentina;* [d]*Institute of Technology Professor J. A. Sábato, Universidad Nacional de San Martín-CNEA, CIC, Buenos Aires, Argentina*

(*Received 9 January 2007; final version received 25 August 2008*)

The effect of different post-weld heat treatments on the microstructure and wear resistance of martensitic deposits were studied. The deposit was welded using a metal-cored tubular wire, in the flat welding position, on a 375 × 75 × 19 mm SAE 1010 plate, using 98% Ar–2% CO_2 shielding gas mixture and with an average heat input of 2.8 kJ/mm. The samples were heat treated at temperatures between 500 and 680°C for 2 h. Chemical composition, Vicker's microhardness and wear properties with AMSLER tests in a sliding condition were determined. In the as welded condition, the microstructure was principally composed of martensite and retained austenite. Significant variations in wear resistance and hardness were measured for different tempering temperatures. For the different heat-treated conditions, it was observed that the decomposition of retained austenite to martensite and carbide precipitation was associated with the tempering of martensite. A secondary hardness effect was detected with maximum hardness of 710 HV for 550°C heat treatment temperature. The best performance in wear test was obtained for this condition. Wear rates for the different conditions were obtained and mathematical expressions were developed. For each case, wear mechanisms were analyzed.

Keywords: hardfacing; martensite; post-weld heat treatment; AMSLER wear test

1. Introduction

Hard-face welding is a commonly used method for functionalizing surfaces subjected to severe wear, corrosion or oxidation, which has transformed itself into a field of broad application and technical development, both in the manufacturing of new components and in the repair and extension of useful life across a vast range of industries[1]. In this context, the systematic study of various consumables and welding processes applied to hardfacing is of great interest for the optimization of the design of the consumables and for the evaluation and fine tuning of the welding procedures. Thus, the heat supply, the type of shielding gas used, the pre-heating temperature or the post-weld heat treatment are some of the variables that affect the characteristics of the deposit[2].

Among welding consumables, tubular wires have recently become one of the most widely used options. These consumables show greater productivity and flexibility in production for alloy grades, constituting an economically advantageous alternative[3]. In particular, metal-cored tubular wires combine advantages of very low slag generation, low fume generation rate and high depositing speeds[4,5]. However, the information in the literature relating to systematic studies on this type of material, in particular hardfacing materials, is scarce.

In general, hard-faced material for applications relating to waste, possess a structure with high hardness or can be hardened through mechanical hardening or heat treatment, such as martensite or a soft matrix with hard particles or second phases (carbides or borides) according to the type of application intended[6]. In particular, for metal–metal hot sliding, the wear is due fundamentally to the mechanisms of abrasion and adhesion, and consequently materials with carbon contents between 0.1 and 0.7 wt% and up to 20% alloying (Cr, Mn, Mo, W and/or V) as martensitic steels for tools or stainless martensitic steels[1,7]. These welding deposits generally require a post-weld heat treatment in order to adjust the final mechanical properties and relieve stress, which has consequences for the component's useful life[8].

The objective of the present work was a systematic study of the effect of pre- and post-weld heat treatment on the wear behaviour and the microstructural evolution of the martensitic weld metal for tools, deposited with a metal-cored tubular wire. To this end, we sought to optimize the said temperature from the point of view of wear resistance, to understand the mechanisms involved and to generate useful information for users and manufacturers.

2. Materials and methods

A hard-faced test piece was welded onto a sheet of 375 × 75 × 19 mm carbon steel type SAE 1010, depositing four layers with the following sequence of 4, 4 and 3 beads in each layer, respectively, as shown

ISSN 0950-7116 print/ISSN 1754-2138 online

DOI: 10.1080/09507110902844071
http://www.informaworld.com

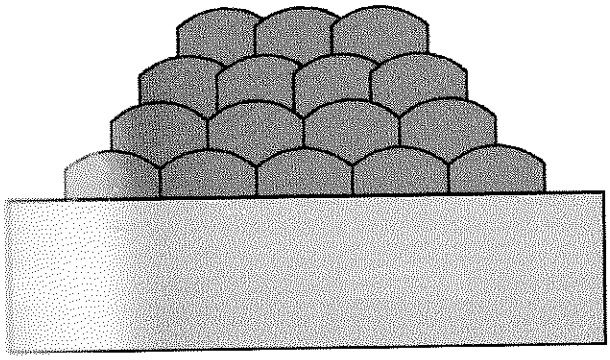

Figure 1. Welding sequence.

in Figure 1. This distribution of layers was selected according to the dimension of the wear test pieces, the possibility of obtaining an undiluted deposit and the operative aspects of the weld.

The consumable employed was a metal-cored tubular wire of diameter 1.2 mm, deposited using the semi-automatic GMAW welding process, using a Railtrac RW1000 automation device. The weld parameters employed can be seen in Table 1.

The free length of the wire was 20 mm and the volume flow of the gas was 18 l/min. It was welded in a flat position and the preheat and between-pass temperatures were 150°C. The welded test piece was X-rayed to evaluate the quality of the deposit.

From the test piece, 12 cross-sections 10 mm thick were extracted, 10 of which were subjected to post-weld heat treatments at 500, 550, 600, 650 and 680°C for 2 h.

On one of the cross-sections obtained, the chemical composition of the final bead was determined by optical emission spectrometry (OES).

For the different conditions studied, the resulting microstructure was characterized using a light microscope (LM) and X-ray diffraction (XRD).

Based on the cross-sections that were heat-treated and in the as welded (AW) condition, test pieces were mechanized for the wear tests. The present material was used as normal in applications associated with metal contact with pure sliding, at temperatures in the range[9] of 20–400°C. In order to evaluate the behaviour under said service conditions, wear tests were carried out on an AMSLER machine[10] under pure sliding conditions, with an applied load of 1250 N. The geometry of the test pieces used can be seen in Figure 2.

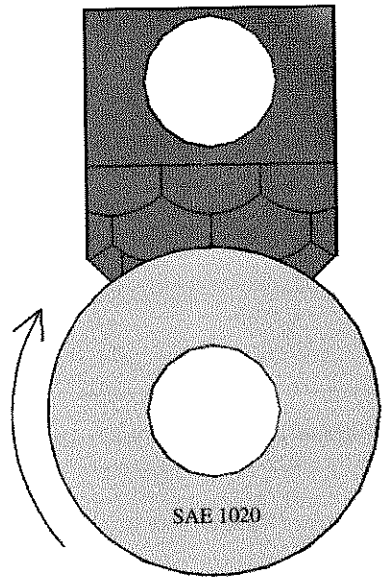

Figure 2. Schema of the wear pair.

The wheel has a radius of $R = 20$ and its rotation speed was 220 rpm. As the reference material, an SAE 1020 steel was used. The surface roughness was measured using a Hommelwerke T1000 rugosimeter in the area of the central line, in the transverse direction to the adjusted direction, for both test pieces (plate and wheel), giving the resulting value of $R_a = 0.8\ \mu m$. Prior to the test, the test pieces were cleaned using ultrasound and were weighed on analytical scales. For each heat treatment and AW condition, the microhardness was measured with 1000 g of applied load (VH 1) in various zones adjacent to the wear surface, as shown in Figure 3.

The wear behaviour was studied according to the distance covered during the sliding of the wheel over the plate, the weight loss being determined for 275, 550, 825, 1100, 1375, 1650, 3300 and 4950 m travelled. For each heat treatment condition, two plate wheel sets were tested, with the results obtained being averaged. The residue produced during each of the intervals was collected. Moreover, due to the friction between the plate and the disk, the temperature of the pair rose during the test. In order to determine the temperature reached in the zone near the wear surface, the temperature was measured after 1 h of continuous testing using a thermocouple located

Table 1. Welding parameters.

Welding gas	Voltage (V)	Current (A)	Forward speed (mm/s)	Oscillation (mm)	Oscillation speed (mm/s)	Heat supply (kJ/mm)
98% Ar–2% CO_2	31	250	2.74	5	60	2.8

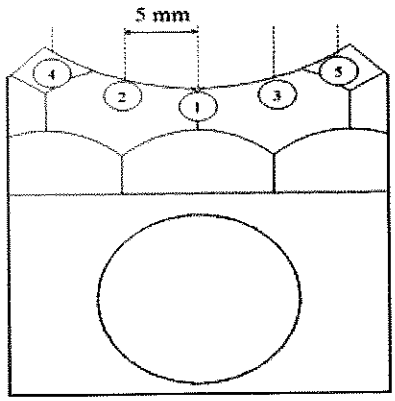

Figure 3. Schema of the surface hardness scan.

on the lateral surface of the plate at 1 mm from the wear surface.

Finally, the wear surfaces as well as the cross-sections were observed using a scanning electron microscope (SEM) in order to determine the wear mechanisms involved and the residue collected was characterized using XRD and SEM.

3. Results and discussion

3.1 *Macrostructure*

In Figure 4(a) can be seen an image of the welded test piece, and in Figure 4(b) a cross-section of the said test piece, showing the base metal, the hard-faced material and the low level of macroscopic defects (pores, slag inclusions, fissures, etc.). For this purpose, the level of defects was evaluated using the ASME IX code, found below the maximum admissible values presented[11].

3.2 *Chemical composition*

Table 2 shows the chemical composition measured on the transverse surface of the final bead, using OES.

It is important to clarify that the chemical composition varies according to the distance from the surface, due to the dilution effect with the base metal. However, as shown in a previous work[12], in the zone corresponding to the wear surface, the chemical composition did not vary significantly.

3.3 *Microstructure*

In Figure 5, the microstructure of the metal deposited can be seen in a cross-section at a distance of 100 μm from the wear surface across the central line of the deposit on the test piece, corresponding to the zone identified as 1 in Figure 3.

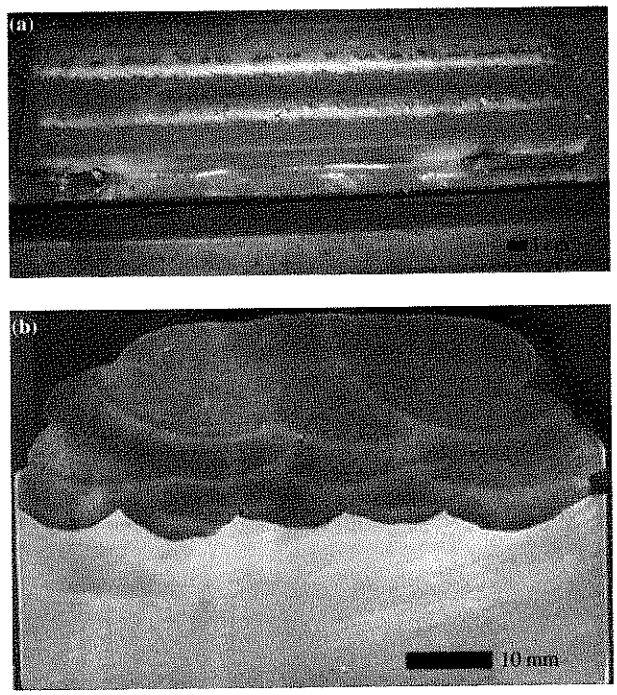

Figure 4. (a) Welded test piece. (b) Cross-section of the welded test piece.

The microstructure for the AW condition (Figure 5(a)) is composed of martensite and retained austenite, with a pattern of dendritic separation: these observations are consistent with what is expected for this type of materials[1–7]. Due to the increased alloying in the inter-dendritic zone[12], a reduction of the start temperature for the martensitic transformation (Ms) occurs, which explains the presence of retained austenite[6]. On the other hand, due to the fact that this was a multi-pass deposit, a tempering of martensite takes place with the successive beads, which would lead to the precipitation of small carbides, which may be of the $M_{23}C_6$ and M_6C type, according to previously reported data[13]. It is reported in the literature that the size of these precipitated carbides is less than 2.5 μm, as a result of which they are not observable with a LM; however, these would be responsible for the darkening observed in martensite.

For the different heat treatment conditions, the decomposition of austenite retained in martensite occurred. As may be seen in Figure 5, as the treatment temperature increased, the fraction of retained austenite observed in the microstructure fell. This is consistent

Table 2. Chemical composition (% by weight).

C	Mn	Si	S	P	Cr	Mo	V	W
0.44	1.20	0.60	0.016	0.02	5.30	2.4	0.34	1.0

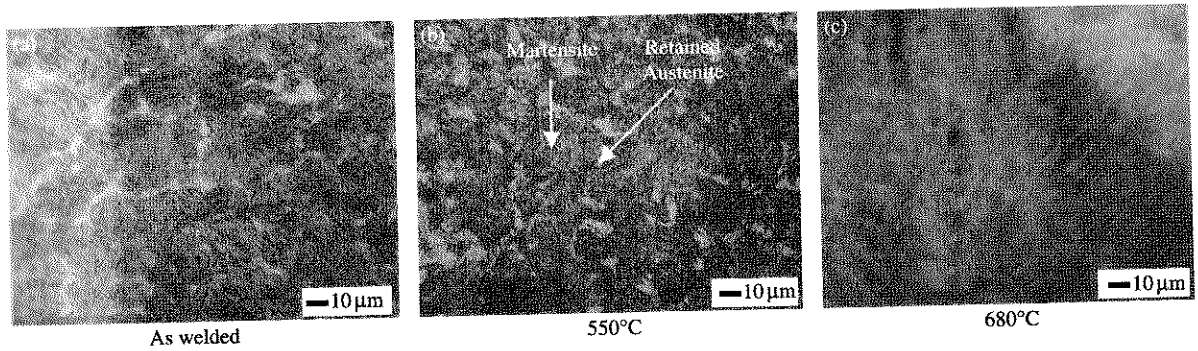

Figure 5. Microstructure of the wear surface for the different heat treatment temperatures.

with the conditions detected in the XRD spectra, where the percentage varied from 16 to 5%, calculated using the peak comparison method[14]. In Figure 6, the spectra obtained for the test pieces in AW condition and with heat treatment of 550 and 680°C are shown.

In turn, in said spectra it is possible to see, for the samples with heat treatment, the presence of carbides of the M_6C type and the reduction of the width and slip of martensite peaks, a product of the stress relief and the reduction of the solute content in the network. The presence of these carbides is increased by the condition of 680°C, associated with greater precipitation. The increase of the martensite percentage was produced at the expense of the austenite transformation in this phase[15].

Wear resistance and microhardness

Figure 7 shows the results obtained from the pure metal–metal sliding wear test. In this Figure, the weight loss according to the distance travelled by the wheel over the plate, for the different heat treatment temperatures is shown.

All the heat treatment conditions, except for 680°C, showed a lower weight loss than the AW condition for 1660 m of distance travelled. As can be seen from Figure 7, the lowest wear occurred for the test pieces treated at 550 and 600°C, with both results being very similar. For the condition of 500°C, a weight loss was noted that was greater than for the aforementioned conditions, but lower than for the AW condition. For the test pieces treated at 680°C, a much greater weight loss was obtained, principally for distances greater than 1660 m.

For the case of the test piece heat treated at 680°C, which showed severe wear, the adjustment was carried out with two expressions, one for the first linear stage (up to 1700 m) and the other for the curve as a whole. In both cases, the R^2 correlation coefficient was greater than 0.99, showing a very good linear adjustment. Based on these results, the wear rate was calculated, obtained from the slope of the straight lines for weight loss and the distance travelled, which for the 680°C condition corresponds to the first stage.

In Figure 8(a),(b), the hardness and wear rate are shown according to the heat treatment temperature.

As can be seen, there is a clear link between the variation in the hardness of the deposit and the wear resistance for that material. The general trend observed is that as the hardness increases, the wear rate decreases. The samples showing the greatest hardness showed the lowest wear rate. This fact may be associated with the precipitation of coherent carbides and the transformation of austenite into martensite during the heat treatment. This fine carbide precipitation gave the metal greater hardness and greater wear resistance. Under these conditions, the control wear mechanism was oxidational[16], as can be seen in Figure 9(a).

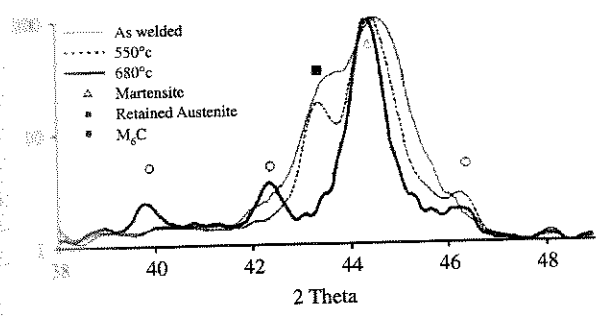

Figure 6. X-ray diffraction spectrum (XDS) of the test pieces with heat treatment.

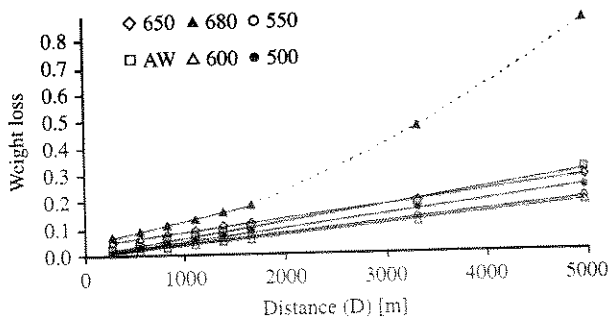

Figure 7. Weight loss as a function of distance travelled.

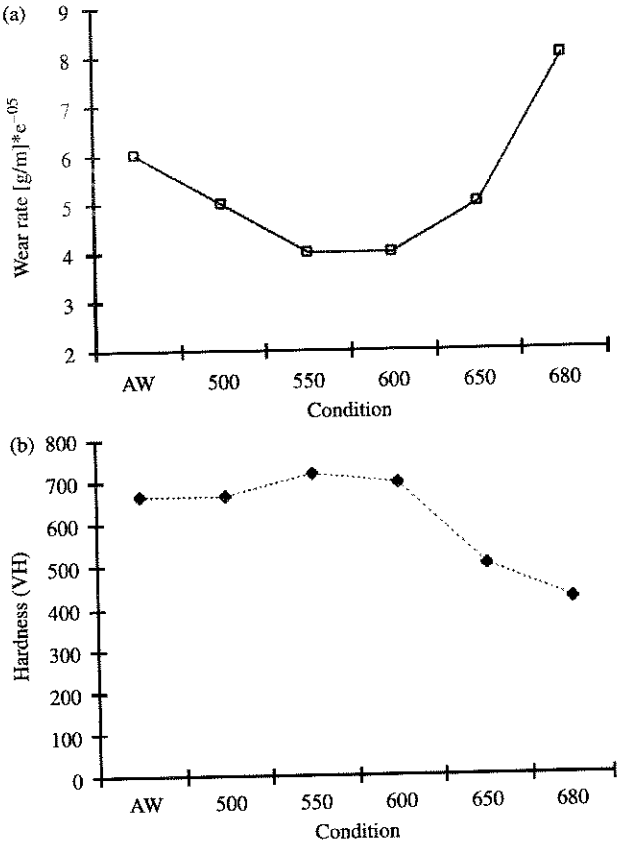

Figure 8. (a) and (b). Wear rate and hardness as a function of the temperature of the heat treatment.

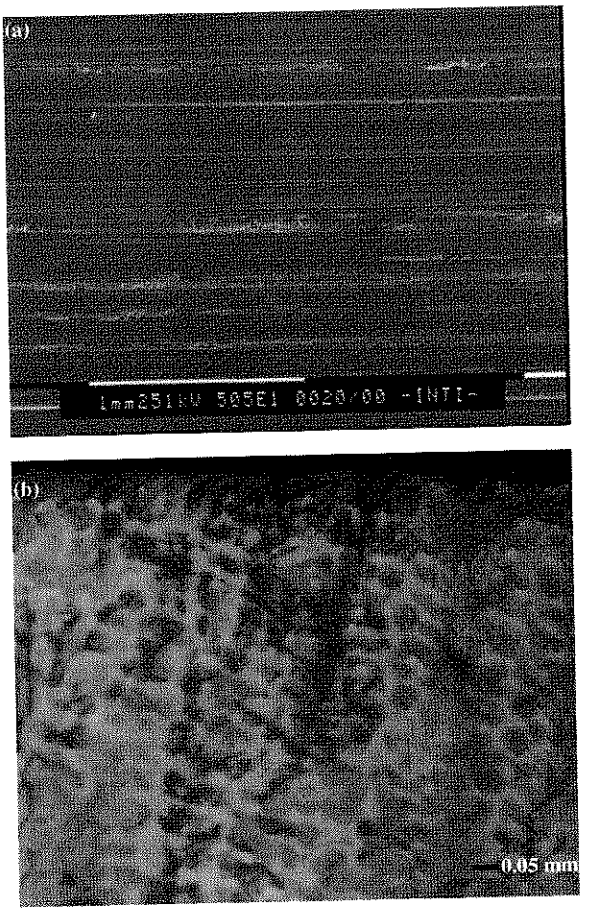

Figure 9. (a) SEM image of the wear surface. (b) Longitudinal section of the wear surface, both corresponding to the test piece treated at 550°C.

It was noted that the hardness on the wear surface was maintained more or less constant between the AW condition and the condition of 500°C heat treatment. This may be related to a compensation between the softening of martensite, due to the loss of carbon, and the hardening produced by the transformation of a part of austenite into martensite and the precipitation of carbides[15–17]. This precipitation would explain the improvement in the wear rate observed for the test piece with heat treatment[16].

For 550 and 600°C, an increase in hardness up to the maximum (710 VH), and a reduction of the wear rate to the minimum value occurred. The secondary hardening effect in this temperature range reached its maximum value, increasing the wear resistance[18].

In Figure 9, the wear grooves on the wear surface obtained after 5000 m of distance travelled can be seen, corresponding to the sample with heat treatment at 550°C. The principal wear mechanisms were oxidative, and to a lesser extent abrasive and adhesive, as can be seen in Figure 9(a).

In Figure 9(b), the microstructure in the zone near to the wear surface on a longitudinal section can be seen, for a test piece treated at 550°C after testing. In this figure, the martensitic microstructure with retained austenite can be seen, as well as zones with martensite needles transformed from the retained austenite. In the vicinity of the contact surface, plastic deformation and a darkening of the structure due to the temperature generated to a depth of about 15 μm below the free surface can be observed.

In Figure 10, the particles of the residue can be seen, shown in two groups according to their size: small (tens of microns) and particles of larger size (hundreds of microns) with a flat morphology, corresponding to the hardfacing material, as determined using EDS.

In the XRD analysis, carried out on the residue (Figure 11), metallic particles and the following oxides were found: Fe_2O_3 and Fe_3O_4. The formation of said oxides was promoted by the elevated temperature in the wear zone, which was approximately 410°C. The presence of these oxides could reduce the wear rate by acting like a protective film, principally the Fe_3O_4 given that said oxide shows high hardness[19–22].

Finally, for higher heat treatment temperatures (650 and 680°C) an abrupt fall in the hardness and a significant increase in the wear rate were observed. These facts may

Figure 10. SEM image of the residue collected for 3320 m of the distance travelled, corresponding to the test piece treated at 550°C.

be associated with the growth and the loss of coherence of the precipitated carbides and the loss of carbon from martensite, which produces a softening of the matrix[17], resulting in an increase in plastic deformation. The greater size of the carbides and the increase in the distance between them also promote adhesion between the surfaces[22–24].

In Figure 12(a), corresponding to the test piece treated at 680°C, delamination was identified as the dominant wear mechanism, and to a lesser extent adhesion and abrasion. On the longitudinal section (Figure 12(b)) of the test piece, we can see a fundamentally martensitic structure, with a deformed zone around the contact surface greater in size than that observed in Figure 9. Oxidation on the wear surface and subsurface fissures were also noted; oxidation was detected within these[25].

In Figure 13, an image of the residue collected for 3320 m of distance travelled is shown, corresponding to the test piece treated at 680°C. It can be seen that the size of the particles is greater (up to 500 μm) than that observed in Figure 10 for the test piece treated at 550°C (up to 100 μm).

Using EDS, larger particles of the hardfacing material and particles corresponding to the reference material, showing plastic deformation, were identified. This increase in size would have produced a reduction in the

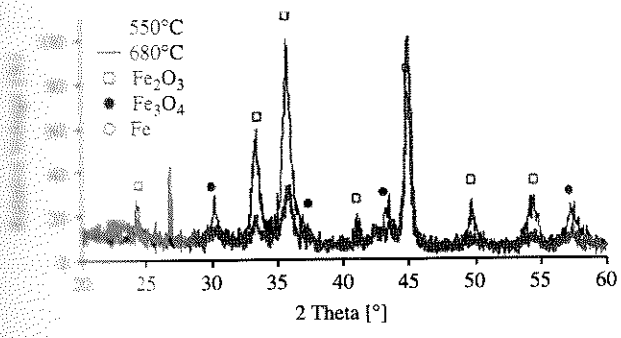

Figure 11. XRD spectral analysis of the residue collected, corresponding to the test pieces treated at 550 and 680°C.

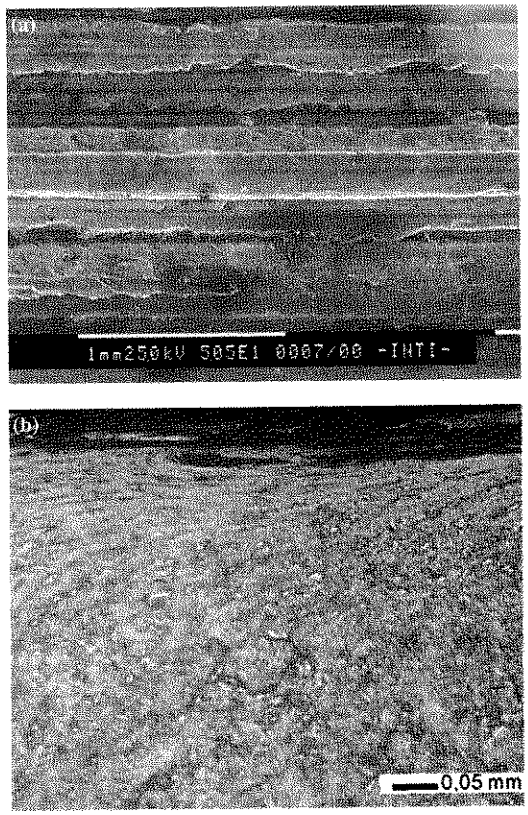

Figure 12. (a) SEM image of the wear surface. (b) Longitudinal section of the wear surface, both corresponding to the test piece treated at 680°C.

lubricating effect between both surfaces with the consequent increase in the wear rate[26].

It should be noted that for heat treatment conditions of 500 and 650°C, the wear rate was similar, while the hardness of the sample treated at 500°C was significantly higher. This may be related to the fact that at 650°C the microstructure was composed of martensite with a lower carbon content and a greater quantity and size of carbides,

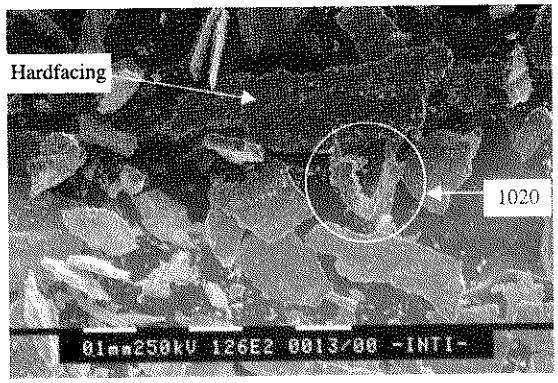

Figure 13. SEM image of the residue collected for 3320 m of the distance travelled, corresponding to the test piece treated at 680°C.

associated with a reduction in hardness, due to the loss of carbon from martensite and the incoherent precipitation of the carbides. However, the wear resistance was maintained, due to the presence of said carbides, which, as previously stated, improve the delamination wear resistance[8,18].

4. Conclusions

The microstructure of the hard-facing material for the AW condition in the contact zone of the test piece was composed principally of martensite and retained austenite. As the temperature of the heat treatment increased to 500°C, it was observed that the austenite fraction decreased until it practically disappeared at 680°C, transforming into martensite and producing the precipitation of M_6C-type carbides.

The wear on the hard-facing test piece under pure sliding conditions in an AMSLER test with a load of 1250 N showed a linear variation between the weight loss and the distance travelled, with expressions obtained that connect these magnitudes for the different conditions. In turn, the wear rate for all cases was obtained. The temperature in the zone near the contact surface (1 mm) for 1 h of testing reached 410°C.

All heat treatment conditions, except 680°C, showed a better wear rate than the AW condition.

A secondary hardening phenomenon was observed with the heat treatment, reaching the maximum hardness (710 VH) at 550°C. For higher temperatures, the hardness fell below the values obtained for the AW condition. A relationship between the variation in hardness and the variation in the wear rate was observed.

The best wear behaviour was shown by the test pieces with heat treatment at 550 and 600°C, which in turn showed the highest hardness. This was associated with the precipitation of coherent carbides, which promote a significant secondary hardening, related to the decomposition of the austenite into martensite and the formation of an oxide layer.

The wear mechanisms observed were oxidation, delamination, abrasion and adhesion. For the heat treatment temperature of 550°C, the principal mechanism was oxidational, showing low wear rates. For the temperature of 680°C, the principal wear mechanism was delamination.

On the wear surface of the hard-facing test piece, a discontinuous layer of oxide and superficial plastic deformation were observed, in a parallel direction to the contact surface and with a darkening associated with the heating of the material. The depth of this deformed zone increased for test pieces with lower hardness.

The residue comprised soft particles of the reference material, hard particles of the hard-facing material and oxides. The size of said particles increased as the hardness of the test pieces analyzed decreased, consistent with the increase in the wear rate and changes in the wear mechanisms in action.

Acknowledgements

The authors would like to thank Eutectic-Conarco for the provision of the consumable used, ESAB Brazil for the production thereof, developed especially for this work, Air Liquide Argentina for the donation of the welding gases, the Industrial Applications Workshop of Conarco-Esab for the welding facilities, Conarco-Esab for the realization of the chemical analyses, the Electron Microscopy Laboratory at INTI-Mecánica for the realization of the scanning electron microscopy, the Amorphous Solids Laboratory for the diffraction spectra and APUENFI (Association of Entrepreneurs-Teachers in the Mechanical Domain of the FI-Universidad Nacional de Lomas de Zamora) for its economic support for the present project. They would also like to acknowledge the ANPCyT for its financial support.

Notes

1. Email: agustingualco@yahoo.com.ar
2. Email: hsvobod@fi.uba.ar
3. Email: esurian@hotmail.com
4. Email: ldevedia@cnea.gov.ar

References

1. Merric S, Kotecki D, Wu J. Surfacing. Welding handbook: materials and applications. Vol. 4. 8th ed. Miami, FL: American Welding Society; 1998. p. 392–435.
2. Bhushan B, Gupta BK. Handbook of tribology: materials, coating, and surface treatment. Malabar, FL: Krieger Publishing Company; 1997.
3. Huisman MD. Flux- and metal-cored wires, a productive alternative to stick electrodes and solid wires. Svetsaren. 1996;51(1–2):6–14.
4. Lyttle KA. Metal cored wires: where do they fit in your future? Weld J. 1996;75(10):35–38.
5. Myers D. Metal cored wires: advantages and disadvantages. Weld J. 2002;81(9):39–42.
6. Wu W, Hwu LY, Lin DY, Lee JL. The relationship between alloying elements and retained austenite in martensitic stainless steel welds. Scripta Materialia. 2000;42: 1071–1076.
7. Kotecki D, Ogborn J. Abrasion resistance of iron-based hardfacing alloys. Weld J. 1995;74(8):269–278.
8. Bortoni OE, Patrone JJ, Marino PS. Recargues por soldadura de superficies sometidas a desgaste [Hardfacing welding of surfaces subject to wear]. Siderurgia. 1989;49:114–139.
9. Hoja de producto: EnDOtec DO*15, de Eutectic Castolin ESAB, Argentina; 1996
10. Battelle WAG. Friction, wear and surface testing. ASM handbook: mechanical testing and evaluation. Vol. 8. 1st ed. Metals Park (OH): ASM International. Handbook Committee; 2003. p. 751–755.
11. ASME IX. Boiler and pressure vessel code. 2004; p. 8–
12. Gualco A, Svoboda HG, Surian E, Ramini M, De Vedia L. Estudio de dilución en depósitos de soldadura para recargues duros [Study of dilution in welding deposits for hardfacing

SAM-CONAMET. Mar del Plata, Buenos Aires, Argentina; 2005.
13. Leshchinskiy LK, Samotugin SS. Mechanical properties of plasma-hardened 5% chromium tool steel deposited by arc welding. Weld Res. 2001;80:25–30.
14. Cullity BD, Stock SR. Elements of X-ray diffraction. 3rd ed. Englewood Cliffs (NJ): Prentice-Hall; 2001.
15. Dobrzanski LA, Mazurkiewicz J, Hajduczek E. Effect of thermal treatment on structure of newly developed 47CrMoWVTiCeZr16-26-8 hot-work tool steel. J Mater Process Technol. 2004;157–158:72–484.
16. Cui XH, Wang SQ, Wang F, Chen KM. Research on oxidation wear mechanism of the cast steels. Wear. 2008; 265:468–476.
17. Verhoeven JD. Fundamentos de Metalurgia Física [Fundamentals of physical metallurgy]. México: Editorial Limusa; 1987. p. 592.
18. Suh NP. An overview of the delamination theory of wear. Wear. 1977;44:1–16.
19. Fontalvo GA, Mitterer C. The effect of oxide-forming alloying elements on the high temperature wear of a hot work steel. Wear. 2005;258:1491–1499.
20. Quinn T, Sullian L, Rowson D. Origins and development of oxidational wear at low ambient temperatures. Wear. 1984; 94:175–191.
21. So H, Yu DS, Chuang CY. Formation and wear mechanism of tribo-oxides and the regime of oxidational wear of steel. Wear. 2002;253:1004–1015.
22. Rodenburg C, Rainforth WN. A quantitative analysis of the influence of carbides size distributions on wear behaviour of high-speed steel in dry rolling/sliding contact. Acta Materialia. in press.
23. Fontalvo GA, Humer R, Mitterer C, Sammt K, Schemmel I. Microstructural aspects determining the adhesive wear of tool steels. Wear. 2006;260:1028–1034.
24. Bahrami A. Effects of conventional heat treatment on wear resistance of AISI H13 tool steel. Wear. 2005;258:846–851.
25. Barrau O, Boher C, Gras R, Rezai-Aria F. Analysis of the friction and wear behaviour of hot work tool steel for forging. Wear. 2003;255:1444–1454.
26. Kato H. Severe-mild wear transition by supply of oxide particles on sliding surface. Wear. 2003;255:426–429.